

1 SEISMIC DESIGN OF SINGLE-STORY PRECAST STRUCTURES FOR 2 P-Δ EFFECTS

3 Marianna Ercolino^a, Crescenzo Petrone^b, Gennaro Magliulo^c and Gaetano Manfredi^c

4 ^aUniversity of Greenwich, Department of Engineering Science, Central Avenue, Medway
5 Campus ME4 4TB Chatham, UK

6 ^bUniversity College London, Department of Civil, Environmental & Geomatic Engineering,
7 Chadwick Building, WC1E 6BT London, UK

8 ^cUniversity of Naples Federico II, Department of Structures for Engineering and
9 Architecture, via Claudio 21, 80125 Naples, Italy

10 **Biography: Marianna Ercolino** is a Senior Lecturer in Civil Engineering at the Department
11 of Engineering Science at the University of Greenwich, London, UK. She has served ACI
12 Italy Chapter as Treasurer and Secretary from 2013 to 2015. She received a PhD in
13 Earthquake Engineering from the University of Naples Federico II, Italy, in 2014. Her
14 research interests are the seismic performance of buildings and infrastructures and non-
15 destructive techniques for structural health monitoring.

16 **Crescenzo Petrone** is a Research Associate at University College London, London, UK. He
17 received his BS, MSc and PhD in Earthquake Engineering from the University of Naples
18 Federico II, Italy, in 2008, 2010 and 2014, respectively. His research interests include the
19 performance of the built environment under different natural hazards, as earthquake and
20 tsunamis.

21 ACI member **Gennaro Magliulo** is an Assistant Professor at University of Naples Federico
22 II, Naples, Italy. He received his BS, MSc and PhD in Structural Engineering from the
23 University of Naples Federico II, Italy, in 1995, 1997 and 2001, respectively. He has served
24 ACI Italy Chapter as Treasurer and Secretary from 2003 to 2012 and as member of the Board

1 of Directors since 2013. His research interests include earthquake engineering and reinforced
2 concrete structures.

3 **Gaetano Manfredi** is the Rector of the University of Naples Federico II, Naples, Italy. He
4 received his BS, MSc and PhD in Structural Engineering from the University of Naples
5 Federico II, Italy, in 1986, 1988 and 1993, respectively. His research interests include
6 earthquake engineering, reinforced concrete structures and masonry structures.

7 **ABSTRACT**

8 A systematic parametric study is performed in order to both (a) investigate the influence of P-
9 Δ effects on the seismic response of RC precast one-story structures and (b) assess the
10 efficiency of the corresponding code provisions. At this aim, different design approaches are
11 considered in order to critically review current design provisions included in current building
12 codes with particular focus on Eurocode 8. Numerical analyses demonstrate the significance
13 of the P- Δ effects on the seismic demand in precast structures in terms of displacement
14 ductility. A modification of the approach of current building codes is proposed, which is
15 demonstrated to ensure both a safer behavior and more economic structures.

16 **Keywords:** P- Δ effects; seismic performance; RC precast structures; Eurocode; seismic
17 design

18 **INTRODUCTION**

19 When a flexible structure is subjected to horizontal actions, i.e. earthquake actions, the
20 gravity loads acting on the deformed configuration lead to a displacement amplification. This
21 is generally referred to as “P- Δ effects”, or geometric nonlinearity. The factors which govern
22 the intensity of P- Δ effects are the magnitude of the gravity loads and the horizontal
23 displacements induced by the earthquake load. In case either the displacement is significant
24 or gravity loads are large, P- Δ effects can lead to structural instability. Therefore, for flexible
25 structures these effects can be vital and they should be appropriately considered during the

1 seismic design of structures, for instance, by increasing the structure stiffness with member
2 oversizing. The described problem is particularly relevant for precast single-story buildings
3 because of the large flexibility of columns. One-story precast buildings consist of precast
4 columns connected at the top by pinned connections. This structural typology is very flexible
5 and the top horizontal displacement can achieve large values under severe seismic actions.
6 Such a structural typology exhibited significant damage after 2012 Emilia earthquake¹⁻³.

7 In the last decades, several authors carried out research studies in order to investigate P- Δ
8 effects on single-story and multi-story buildings. Firstly, research studies focused on defining
9 when P- Δ effects are negligible^{4, 5}. In these works, the authors defined whether P- Δ effects
10 had to be considered by means of a stability coefficient approach; i.e. some limit values of
11 these coefficients were proposed. The stability coefficient mainly depends on the lateral
12 stiffness of the structure, the ductility demand, and the axial loads. Bernal⁶ and MacRae⁷
13 studied this topic and both the authors proposed considering P- Δ effects by increasing the
14 strength of the structure in order to have the same ductility demand as in the structural
15 response without P- Δ effects. In Bernal⁶ the amplification factor was defined as the ratio of
16 the strength required to a SDOF system in order to have a given peak displacement ductility
17 demand, with and without P- Δ effects. This amplification factor was strictly correlated to the
18 stability coefficient and displacement ductility; on the contrary, there was no significant
19 correlation of this factor with the structural period. In this study, the stability factor, θ , is
20 defined as the ratio between the axial load and the product of the lateral stiffness and the
21 structure height. MacRae⁷ demonstrated that the hardening ratio is the most significant
22 parameter in the study of P- Δ effects since this parameter controls the cumulative inelastic
23 deformation and the likely dynamic instability due to the geometric nonlinearity. Recently,
24 Amara et al.⁸ proposed an accurate analytical definition of the strength amplification factor as
25 a function of the kinematic ductility, the interstory drift sensitivity coefficient and the

1 equivalent viscous damping ratio of the system. Similarly to the other amplification factors,
2 this proposed coefficient should compensate the influence of P- Δ effects in the response of
3 SDOF systems. Humar et al.⁹ showed that P- Δ effects cause the dynamic instability of the
4 structure if the post-elastic stiffness becomes negative and in this case the amplification of
5 either the strength or the stiffness does not ensure stability. In a single-story structure, a
6 sufficient strain hardening (i.e., larger than the stability factor, θ) can ensure stability since
7 the post-yielding stiffness is positive even in presence of P- Δ effects. In a multi-storey
8 structure, there is no need to strengthen the structure for P- Δ effects if the displacement is in
9 the positive slope of the force–displacement relationship, obtained by a pushover curve.
10 Some research studies criticized the use of the stability coefficient and alternative methods
11 were proposed. Some examples of these works are described in the following. The use of the
12 conventional stability coefficient (θ) may require several iterations to converge in the final
13 design, because, for instance, the initial stiffness is unknown in the initial design phase.
14 Moreover, the stability coefficient neglects some important factors for the seismic safety of
15 structure, such as the shape of the controlling mechanism. In their work, Aschheim and
16 Montes¹⁰ used the Yield Point Spectra in order to evaluate the influence of P- Δ effects on the
17 lateral strength associated to constant ductility demands. The proposed design approach
18 provided the estimation of the yield displacement by means of the effective height, h_{eff} ,
19 representing the magnitude of P- Δ effects. The advantage of this method is that both the
20 effective height and the yield displacement may be estimated in the design phase and they are
21 quite stable parameters, as the initial design concept is refined into the final design.

22 RESEARCH SIGNIFICANCE

23 Current building codes^{11, 12} consider P- Δ effects according to some of the above-described
24 research studies. The influence of P- Δ effects can be relevant for precast industrial buildings,
25 as it typically leads to a significant member oversizing during the design phase. Literature

1 research studies typically focused on theoretical models, i.e. generic SDOF systems, rather
2 than on real buildings, designed according to the code provisions. The paper aims to assess
3 the reliability of the current approach included in building codes, with particular focus to
4 Eurocode 8¹¹, to evaluate the influence of P- Δ effects on the design of single-story precast
5 buildings. The EC8 provisions are adopted in the design of the case-studies, such as the code
6 amplification factor and the minimum size of vertical elements.

7 **METHODOLOGY**

8 An extensive parametric study is performed on single-story precast structures by varying
9 both the structural geometric features and the seismicity level of the site. The influence of P-
10 Δ effects is extensively assessed for the defined case-studies by means of nonlinear dynamic
11 analyses, as in Bernal⁶ and Humar, Mahgoub⁹. Each EC8¹¹ provision, used in order to take
12 into account P- Δ effects, is investigated and alternative design approaches are assessed by
13 comparing their results with the standard code approach.

14 Most of precast industrial structures consist of one-story buildings with slender columns,
15 connected with socket foundations at the base (Fig. 1). Such a connection can ensure a fixed
16 joint at the column base in case the embedded length of the column is adequate (1.5 times the
17 column size), as demonstrated in past works^{13, 14}. The columns are connected to the beams by
18 means of pinned connections (dowel connections), i.e. the flexural stiffness of the connection
19 is very low. This connection is the most typical one in precast buildings and it is also the
20 most critical for P- Δ effects because of the large flexibility of the buildings under seismic
21 actions. For this structural typology, the columns can be modelled as a SDOF system (Fig. 2),
22 characterized by their lateral stiffness and by a mass evaluated from a tributary area
23 approach.

1 **Parametric study: selection of the structures**

2 The case-studies are defined by varying both the height of the structure and the total seismic
3 mass. The assumed values represent a set of realistic single-story precast structures: four
4 values of the column height H , from 6 m to 12 m (19.7 ft-39.4 ft) and eight values of the
5 mass m , from 10 t to 150 t (22046 lb-330693 lb) are considered. These mass values reflect
6 realistic spans and vertical (permanent and live) loads in precast structures. The minimum
7 value is typical of small dimension structures without roof concrete slab. The maximum value
8 is typical of large dimension structures with a roof concrete slab of 5 cm (1.97 in). Moreover,
9 three design peak ground accelerations, a_g , are considered: 0.15 g, 0.25 g and 0.35 g. The
10 total number of investigated structures is equal to 96. The case studies refer to a soil type B,
11 characterized by an average shear wave velocity $V_{s,30}$ in the range 360 m/s and 800 m/s
12 (1181 ft/sec-2625 ft/sec), according to EC8.

13 Each column of the case-study has a square cross-section and is designed according to
14 European Building Codes EC2¹⁵ and EC8. A modal response spectrum analysis is performed
15 and the behavior factor is assumed equal to 3.5, according to the prescription by Italian
16 Building Code¹⁶ for ductility class high for single-story precast structures. The Damage
17 Limitation (DL) limit state is satisfied by restricting the inter-story drift to 1% for a frequent
18 earthquake, according to the procedure recommended by EC8 for importance class II.

19 The steel reinforcement has a yield characteristic strength of 450 MPa (9398 kips/ft²),
20 whereas the concrete characteristic compressive cylinder strength is equal to 45 MPa
21 (939.8 kips/ft²). The code design values are used in the design phase. In the design phase, the
22 column elastic stiffness is assumed equal to half of the corresponding gross stiffness to take
23 into account the effect of cracking; the period of the structure is evaluated as $T = 2\pi\sqrt{m/k}$,
24 where k is the lateral stiffness of a cantilever scheme. The influence of P- Δ effects on the
25 seismic response is evaluated by means of the stability coefficient, θ , according to the EC8:

$$\theta = \frac{P}{H} \cdot \frac{d_r}{V} \quad (1)$$

In Eq.1 P is the gravity load, V is the total seismic shear, H is the story height and d_r is the design inter-story drift. EC8 provides different prescriptions depending on the value of this factor, which are summarized in Table 1. P- Δ effects are taken into account if θ is larger than 0.1: if θ is smaller than 0.2 the seismic effects should be amplified by a factor, α ; the stability factor cannot exceed 0.3. It should be noted that a similar approach is also found in ASCE 7¹², where the stability factor cannot exceed 0.25. If θ is larger than 0.1 in EC8, the cross-section dimensions of primary seismic columns should not be smaller than one tenth of the larger distance between the point of contraflexure and the ends of the column, i.e. the shear span. In the following, this code provision is called “H/10 rule”, because the column shear span corresponds to the column height in the investigated structural typology. It should be noted that Eurocode does not provide any prescription in case θ is in the range 0.2 and 0.3; in this study, the structures are designed following the prescriptions of precast structures characterized by θ larger than 0.1, i.e. amplification of the seismic effects and minimum dimensions of the columns.

16 **Parametric study: design approaches**

17 Four different design approaches (Table 2) are conducted to evaluate the influence of each
18 design provision about second order effects. In particular:

- 19 - Design approach no. 1 → the structures are designed according to all the design
20 provisions included in Eurocode 8 for P- Δ effects.
- 21 - Design approach no. 2 → the structures are designed by neglecting the limit about the
22 minimum cross-section dimension of columns if θ is larger than 0.1 (H/10 rule).
- 23 - Design approach no. 3 → the structures are designed similarly to design no. 2, also
24 neglecting the limit on the maximum value of the stability factor ($\theta = 0.3$).

- 1 - Design approach no. 4 → the cross-sections of the columns designed in the third
2 approach are used and the reinforcement is designed by neglecting P-Δ effects, i.e.
3 without multiplying the seismic effects by the factor α .

4 The results of the different design approaches are shown in Table 3 for each height and peak
5 ground acceleration and for some values of mass for the sake of brevity. The table includes
6 the column cross-section dimension (h); the geometric ratio of the longitudinal reinforcement
7 (ρ); and the stability coefficient (θ). The cells of Table 3 have different background colors in
8 order to inform the reader about the factor that mostly influenced the design. In particular,
9 white background is used if the DL limit state influenced the design of the column sections.
10 Light grey background is used if the limit of the minimum column section influenced the
11 design, i.e. H/10 rule; it is worth noting that in this case the cross-section dimension can be
12 smaller than one tenth of the column shear span since the increase of the cross-section may
13 cause θ smaller than 0.1. Dark grey background is used if the section dimensions were
14 increased because θ was larger than 0.3. Dashed background is used if the section was
15 increased because ρ was larger than the maximum limit value (4%). For the sake of brevity,
16 the results of design approach no. 4 are not shown in Table 3; they differ from the results of
17 design approach no. 3 only in terms of longitudinal reinforcement ratio (ρ). In particular, the
18 reinforcement ratio (ρ) decreases for the structures designed for 0.15 g up to 36% for the
19 highest structures (10 m and 12 m). The reinforcement ratio (ρ) does not change in most of
20 the cases with more severe seismic actions. Some conclusions can be drawn according to the
21 results of the four design approaches.

- 22 - The limitation of the minimum column dimension (H/10 rule) influenced the design
23 of most of the structures of approach no. 1 and this design provision leads to
24 significantly oversized structures¹⁷, particularly for low a_g values.

- 1 - As expected, the column sections of design approach no. 2 are equal or smaller than
2 the sections of design approach no. 1. For low seismicity ($a_g = 0.15$ g) the mean ratio
3 between the cross-section dimensions of approach no. 1 and approach no. 2 is equal to
4 1.24. The absence of the section limitation (H/10 rule) causes a low stiffness and, as a
5 consequence, a large value of θ (which might exceed 0.3, requiring an increase in
6 column cross section). A similar ratio is found for tall structures, i.e. 10 m and 12 m
7 (32.8 ft and 39.44 ft), at higher seismicity ($a_g = 0.25$ g); in these cases, θ is smaller
8 than 0.3 and the DL limitation influences the section dimensions. For the highest a_g
9 value (0.35 g), the difference between the two approaches is small: in approach no. 1,
10 even if the section was defined by the H/10 rule, the final column dimension is only
11 slightly larger than the dimension required by DL limit state.
- 12 - Structures designed according to approach no. 3 have the same features (section and
13 reinforcement) of the structures designed with approach no. 2 for $a_g = 0.25$ g and
14 $a_g = 0.35$ g. For $a_g = 0.15$ g, cross-section designed according to approach no. 3 are
15 about 30% smaller than approach no. 2, while the reinforcement ratio is increased of
16 about 50%. These differences are caused by the different factors influencing the
17 design: for approach no. 2, the governing rule typically is the need to re-design in case
18 θ is larger than 0.3; for approach no. 3 the governing rule typically is the 4%
19 limitation on maximum longitudinal reinforcement ratio.
- 20 - Sensibility coefficient θ is smaller than 0.2 for 0.35 g for the different considered
21 approaches; for 0.25 g, it is in the range 0.1÷0.3 for approaches no. 2 and no. 3, while
22 it is much smaller for approach no. 1. Large values of θ are recorded for approach no.
23 3 for $a_g = 0.15$ g; in this case θ is larger than 0.3 for almost all the structures. This
24 phenomenon is caused by the fact that the smaller the peak ground acceleration, the

1 smaller the stiffness; this evidence confirms the conclusion in Andrews¹⁸ that P- Δ
2 effects are more influent in low seismic prone areas.

- 3 - A further observation concerns the fundamental period of vibration of buildings. By
4 moving from approach no. 1 to approach no. 3, the elastic stiffness decreases and,
5 consequently, the fundamental period increases. The period is larger than 2.0 s only
6 for some structures designed for approach no. 3 for $a_g = 0.15$ g. For such long periods,
7 the design spectral acceleration is kept constant to 0.20 times a_g value, as prescribed
8 by EC8.

9 **Modelling**

10 The four different design approaches are compared by means of nonlinear dynamic analyses.
11 The buildings are modelled as SDOF systems and a lumped plasticity approach is used to
12 simulate the nonlinear behavior of the column. The plastic hinges are assigned at the base of
13 the vertical elements. The columns are modeled with a stiff element and they are fixed at the
14 base. The nonlinear model does not take into account the steel bar strain penetration effects in
15 the valuation of the rotation at the base of the column. This assumption can underestimate the
16 drift under seismic actions¹⁹. A moment–rotation envelope is assigned at the base of the
17 SDOF system, which is idealized into a bi-linear relationship: an elastic-plastic envelope with
18 post-yield hardening is adopted. The values of the yield and ultimate bending moment, M_y
19 and M_u , are evaluated with a fiber analysis on the section. The yielding curvature is defined
20 as the minimum curvature at which the first steel fiber reaches the yielding strength or the
21 first concrete fiber reaches the compressive strain in the concrete at the peak stress, ϵ_{c1} . In the
22 fiber analysis the concrete confinement due to stirrups is considered, according to Mander,
23 Priestley²⁰. Empirical formulas (Eqs. 2 and 3) are adopted for yielding and ultimate chord
24 rotation, as proposed by Fardis and Biskins²¹. The terms in the following equations are
25 defined in the reference paper for the sake of brevity.

$$\theta_y = \phi_y \cdot \frac{L_V + a_{VZ}}{3} + 0.00135 \left(1 + 1.5 \frac{h}{L_V} \right) + \frac{\varepsilon_y}{d-d'} \cdot \frac{d_b f_y}{6\sqrt{f_c}} \quad (2)$$

$$\theta_u = \frac{1}{\gamma_{el}} 0.016 \cdot (0.3^v) \left[\frac{\max(0.01; \omega t)}{\max(0.01; \omega)} f_c \right]^{0.225} \left(\frac{L_V}{h} \right)^{0.35} 25^{\left(\alpha \rho_{sx} \frac{f_{yw}}{f_c} \right)} 1.25^{(100\rho_d)} \quad (3)$$

3 Ultimate bending moment and rotation allow computing the model post-yield hardening.

4 Mean values of material (steel and concrete) strength are used in the nonlinear analyses. They
5 are evaluated according to Eurocode 2¹³ and Eurocode 8-2 prescriptions^{15, 22}. The geometrical
6 nonlinearities are the unique source of degradation in the moment-curvature envelope. Such
7 an assumption is consistent with the main aim of this paper, i.e. to assess the influence of
8 code provisions for P-Δ effects on the seismic response of precast structures. Both the design
9 approaches and the adopted nonlinear model lead to two important considerations, as follows.

- 10 - The value of the fundamental period of vibration in the design phase is significantly
11 smaller than the period of the nonlinear model. The former is evaluated referring to
12 the gross section elastic stiffness of the cantilever scheme reduced by a 0.5 factor,
13 taking into account the section cracking, because of the low values of axial loads in
14 this type of structures; on the contrary, the period in the nonlinear analyses is
15 evaluated from the moment-rotation relationship, i.e. according to the secant stiffness
16 at the yielding point.
- 17 - During the design phase, both the code provisions and the material overstrength could
18 cause an overall structural overstrength, due to seismic detailing rules. For instance, in
19 the design phase the design mechanical features are adopted for the materials, while
20 the corresponding mean values are used in the dynamic analysis. According to
21 Fardis²³, the code provision can lead to an overstrength equal to approximately 1.5 for
22 reinforced concrete frames. This value can be larger in case of low seismic intensity
23 and tall buildings because of specific seismic detailing, e.g. H/10 rule and minimum
24 reinforcement ratios.

1 In order to study the influence on the outcomes of the study of both the shift of fundamental
 2 period and the design overstrength, three different nonlinear models are defined for the
 3 plastic hinge at the column base. In particular, three moment-rotation envelopes are defined
 4 (Fig. 3).

5 - Modeling approach a: the elastic stiffness, k_{el} , of the moment-rotation envelope is
 6 evaluated from the properties of column section as M_y/θ_y . Yield and ultimate
 7 rotation and bending moment are evaluated as described above (black solid line in
 8 Fig. 3).

9 - Modeling approach b: the initial stiffness of the moment-rotation envelope is set
 10 equal to the stiffness assumed during the design phase (black dash-dot line in Fig. 3):
 11 the phenomenon of the period shift is therefore removed. The yielding moment and
 12 hardening are assumed equal to the corresponding values in the modeling approach a;
 13 the yielding rotation is derived from the yielding moment and the assumed elastic
 14 stiffness as: M_y/k_{el} .

15 - Modeling approach c: the elastic stiffness is the same as in modeling approach b and
 16 the yielding moment is evaluated from the design acceleration spectrum (gray solid
 17 line in Fig. 3). Given the design acceleration, S_{ad} , which corresponds to the
 18 fundamental period of vibration T_1 , the bending moment is evaluated as follows:

$$19 \quad \mathbf{M}_y = \begin{cases} \mathbf{S}_{ad}(T_1) \cdot \mathbf{m} \cdot \mathbf{H} & \text{per } \theta \leq 0.1 \\ \mathbf{S}_{ad}(T_1) \cdot \mathbf{m} \cdot \mathbf{H} \cdot 1/(1 - \theta) & \text{per } 0.1 < \theta < 0.3 \end{cases} \quad (4)$$

20 The bending moment is amplified by the coefficient $1/(1 - \theta)$ if P- Δ effects were
 21 considered in the design phase; in this way, the modeling approach c removes all the
 22 overstrength sources (e.g., materials and code detailing provisions) and it takes into
 23 account only the overstrength due to geometric nonlinearities. The evaluated
 24 overstrength values are always larger than 1.5 and they can assume values up to 5 for

1 low seismic intensity ($a_g=0.15g$ and $H=12m$). The hardening is assumed equal to the
2 values in the other models.

3 Finally, it should be underlined that the behavior of the connections among members, e.g.
4 beam-to column connections²⁴⁻²⁶, are neglected and assumed to be infinitely strong and stiff.
5 Moreover, any influence of bidirectional loading on the behavior of RC elements^{27, 28} is not
6 taken into account here.

7 **Input selection**

8 The main goal of the study is the verification of the code approach, used to take into account
9 P- Δ effects during the design of RC precast structures. At this aim, fifty artificial acceleration
10 time histories for the dynamic analyses are selected and scaled in order to match the elastic
11 code spectrum at the three a_g values for soil type B. The generation was performed by means of
12 the SIMQKE program²⁹. The spectrum compatibility is requested in a wide period range
13 ($0.12 \div 6.0$ sec) in order to cover all the possible periods of the case studies¹¹. Fig. 4 shows
14 the elastic spectra of the fifty selected records, scaled in order to match the design elastic
15 spectrum at $a_g = 0.35$ g. In this figure, the average spectrum of the records (solid blue line) is
16 reported along with the design target spectrum (solid black line) and the period range of
17 spectrum compatibility (dashed red lines).

18 **Analysis**

19 Nonlinear dynamic analyses are performed for all the case studies described in the previous
20 sections with the above described accelerograms. As a consequence, 115,220 analyses are
21 performed: the 96 considered case studies are designed according to the four design
22 approaches; they are modelled according to three modeling approaches and the dynamic
23 analyses are performed by both neglecting (1st order analysis) and considering P- Δ effects
24 (2nd order analysis) with 50 accelerograms. For SDOF systems subjected to a ground
25 acceleration $\ddot{a}_s(t)$, the equation of motion is:

$$1 \quad m\ddot{u} + b\dot{u} + k_0u = -m\ddot{a}_s(t) \quad (5)$$

2 where m is the mass of the oscillator, b is the damping coefficient (the damping ratio
3 $b/2\sqrt{k_0m}$ is assumed equal to 0.05), k_0 is the first order elastic stiffness, u , \dot{u} and \ddot{u} are the
4 relative displacement, the relative velocity and the relative acceleration of the system,
5 respectively. Newmark's method³⁰ is adopted and an algorithm is implemented in the
6 program Matlab^{®31} to solve the equation of motion.

7 Second order effects can be taken into account by decreasing the elastic first order stiffness
8 through a parameter, known as geometric stiffness, k_G , which is evaluated as the ratio of the
9 axial force and the height of the system⁸. The ratio of the geometric stiffness and first order
10 stiffness is the stability coefficient θ . The equation of motion changes when P- Δ effects are
11 considered as follows:

$$12 \quad m\ddot{u} + b\dot{u} + (k_0 - k_G)u = -m\ddot{a}_s(t) \quad (6)$$

13 When the structure experiences nonlinear displacements, the equation of motion can be
14 solved at each time increment by replacing the elastic stiffness, k_0 , with the tangent stiffness,
15 r_0k_0 , where r_0 is the hardening ratio. The geometric stiffness remains constant, even if
16 nonlinearity develops in the SDOF system. The presence of P- Δ effects changes the moment-
17 rotation envelope during the dynamic analyses; the moment-rotation envelope in first order
18 analysis is reported in Fig. 5 with solid line while the corresponding behavior in case second
19 order effects are taken into account is shown with dashed line. V_{yp} is the reduced yielding
20 force due to the second order effects.

21 **RESULTS AND DISCUSSION**

22 In this section, the results of nonlinear dynamic analyses are presented for the above-
23 described case studies. The first section ("Strength vs ductility demand") shows the
24 comparison between the first order analysis and the second order analysis to establish the

1 structural demand parameter mostly influenced by P- Δ effects. In order to study the influence
2 of the geometric nonlinearities, the three modeling approaches are compared in terms of
3 ductility demand and the effect of structural overstrength is evaluated (“Influence of the
4 design overstrength and stiffness”). The following sections discuss about the efficiency of the
5 code design provisions used to take into account the P- Δ effects: the limitation on the column
6 dimension (H/10 rule) and the limitation of the stability factor ($\theta > 0.3$). The Section “Design
7 approach no. 4: P- Δ not taken into account” shows the results of the nonlinear dynamic
8 analyses on the case studies, designed according to design approach no.4, i.e. neglecting P- Δ
9 effects provisions. In the last Section (“When are P- Δ effects important?”) the comparison
10 between the analyses with and without P- Δ effects are presented and discussed.

11 **Strength vs ductility demand**

12 In this section, the influence of P- Δ effects on the seismic response of the investigated
13 structures is assessed by comparing the outcomes of nonlinear dynamic analyses. In
14 particular, the force-displacement curve for the first order analysis (black dashed line in Fig.
15 6) is compared to the corresponding curve for second order analysis (gray solid line in Fig.
16 6), considering a single case study, i.e H = 8 m, m = 50 t, $a_g = 0.35$ g (H = 26.2 ft,
17 m = 110231 lb, $a_g = 0.35$ g). Such a case study is designed according to design approach
18 no. 1 and modelled by adopting modeling approach a. The comparison in Fig. 6 leads to the
19 following conclusions:

- 20 - the values of the elastic stiffness in the two analyses are different;
- 21 - the maximum displacement in case P- Δ effects are taken into account is larger than
22 one recorded in the first order analysis;
- 23 - smaller value of shear force is recorded in the second order analysis.

24 In the following the influence of P- Δ effects is performed in terms of ductility demand rather
25 than in terms of demand forces⁸.

1 **Influence of the design overstrength and stiffness**

2 This section describes a comparison between the adopted modeling approaches when second
3 order analyses are performed. Fig. 7 shows the average value of displacement ductility
4 (maximum/yielding) demand versus the mass for all the structures designed according to
5 design approach no. 1. The yielding displacement is defined as the value of the yielding
6 rotation at the column base times the column height. The maximum displacement is defined
7 as the maximum displacement recorded during the nonlinear dynamic analysis at the column
8 top. In particular, each row in Fig. 7 refers to structures with the same height (H) and each
9 column refers to structures designed for the same peak ground acceleration on stiff soil (a_g).
10 The continuous line indicates the results of modeling approach a, the dash-dotted line reports
11 the results of modeling approach b, while dotted line refers to modeling approach c; in these
12 plots, the displacement ductility capacity is also showed with a black dashed line and it is
13 evaluated according to Italian building code¹⁴ as:

$$14 \quad \mu_d = \begin{cases} \mathbf{q} & \text{if } T_1 \geq T_C \\ \mathbf{1} + (\mathbf{q} - \mathbf{1}) \cdot \frac{T_C}{T_1} & \text{if } T_1 < T_C \end{cases}, \quad \mu_d \leq 5\mathbf{q} - 4 \quad (7)$$

15 In these equations, q is the behavior factor, T_l is the fundamental period of vibration and T_C is
16 the corner period. For all the structures, T_1 is larger than T_C and the ductility capacity is
17 always equal to 3.5, i.e. the value of the behavior factor used in this study, according to the
18 equal-displacement rule.

19 The curves show that overstrength has the most important role in the seismic response of the
20 structures: the displacement ductility demand significantly increases if modeling approach c
21 is adopted (dotted line in Fig. 7). Moreover, in this case, the demand is very close to the
22 capacity; on the contrary, the demand for the other two approaches is significantly lower than
23 the capacity. Less significant differences are recorded between the results with the modeling
24 approach a (solid lines in Fig. 7) and the ones with the modeling approach b (dash-dotted

1 lines in Fig. 7), denoting a smaller influence of the fundamental period of the structure
2 compared to structural overstrength. The largest values of overstrength refer to structures
3 designed for $a_g = 0.15$ g; in this case, the ductility demand in modeling approach a is about
4 81% smaller than in modeling approach c. For $a_g = 0.25$ g and 0.35 g, the discrepancy is
5 about 70% and 62%, respectively. This is caused by the design prescriptions on seismic
6 detailing, which give a larger influence for low a_g .

7 **Influence of the code geometric minimum requirements**

8 In this section, the influence of the H/10 rule is investigated by comparing the results of the
9 second order dynamic analyses on structures designed according to different approaches and
10 modeled with the approach c. Average values of the displacement ductility demand of
11 structures designed according to design approach no. 1 (blue line) and no. 2 (red line) are
12 shown in Fig. 8. In these plots the different line typologies refer to the three values of
13 seismicity: solid line for $a_g = 0.15$ g, dashed line for $a_g = 0.25$ g and dotted line for
14 $a_g = 0.35$ g. It should be noted that some curves in Fig. 8 are superimposed, as expected from
15 the outcomes discussed above. For instance, tall structures designed according to approach
16 no. 1 are not influenced by the design peak ground acceleration; hence, curves for different a_g
17 of approach no. 1 (blue lines in Fig. 8) are superimposed for $H = 10$ m and $H = 12$ m. Similar
18 conclusions can be drawn for structures with $H = 8$ m, designed according to approach no. 1
19 for $a_g = 0.15$ g and 0.25 g. There is no change between structures of 6 m and 8 m tall
20 designed according to approaches no. 1 and no.2 for $a_g = 0.35$ g, and between structures of
21 6 m tall designed according to approaches no. 1 and no. 2 for $a_g = 0.25$ g and mass values
22 larger than 30 t. Comparing the results of the two design approaches (no. 1 and no. 2), the
23 following conclusions can be stated.

- 24 - For the lowest peak ground acceleration ($a_g = 0.15$ g), passing from approach no. 1 to
25 approach no. 2, the ductility demand decreases for almost all the structures. This

1 result is mainly justified by the increase of the coefficient α ; as observed in Table 3,
2 the values of the stability factor θ are close to 0.30 for design approach no. 2, then α is
3 about 1.40, and the yield moment increases of about 40%.

- 4 - The reduction of the ductility demand is larger for tall structures. This phenomenon
5 may be justified considering that period elongation due to geometric nonlinearities in
6 tall structures, characterized by a fundamental period close to 2sec, does not cause a
7 significant displacement demand increase. For short-to-medium period structures the
8 displacement increase is much more significant, given the shape of the code spectrum.

9 It can be concluded that the H/10 rule significantly influences the design of precast structures,
10 leading to more expensive buildings without improving their seismic safety.

11 **Maximum acceptable value of θ**

12 Eurocode requires to re-design columns if θ is larger than 0.3; design approach no.3 neglects
13 this prescription and it takes into account geometric nonlinearities only by multiplying the
14 seismic effects by the factor α if θ is larger than 0.1. The displacement ductility demand for
15 this approach (red line) is plotted in Fig. 9 and compared to the results of design approach
16 no. 1 (blue line). The results refer to the modeling approach c with second order analyses.

17 It is worth noting the coincidence of results with approach no. 1 and no. 3 for structures with
18 $H = 6$ m (19.7 ft) and 8 m (26.2 ft) subjected to $a_g = 0.35$ g. However, the ductility demand in
19 approach no. 3 is generally smaller than the demand for approach no. 1. In design approach
20 no. 3, the overstrength is due to the amplification coefficient α and this overstrength
21 decreases for higher peak ground acceleration, because of the lower values of stability factor.

22 Hence it can be concluded that structures designed without any upper bound on the stability
23 coefficient are safer than structures designed according to current building code. The large
24 value assumed by the factor α for θ larger than 0.30 leads to such a conclusion, which is
25 certainly counterintuitive: a less prescriptive building code leads to safer structures. Finally, it

1 should be underlined that for some structures an additional source of overstrength is caused
2 by the prescription on the minimum design spectral acceleration, which cannot be smaller
3 than 0.20 times a_g . Therefore, for long period structures, the corresponding spectral
4 acceleration in the nonlinear analysis is lower than the value assumed during the design
5 phase.

6 **Design approach no. 4: P- Δ not taken into account**

7 The last design approach does not take into account P- Δ effects. The cross-section
8 dimensions designed in approach no. 3 are used and the longitudinal reinforcement ratio, ρ , is
9 specifically evaluated. The comparison between the displacement ductility demand of
10 approaches no. 1 (blue line) and no. 4 (red line) is presented in Fig. 10. As in previous
11 sections, the results refer to modeling approach c and to second order analysis; different lines
12 typologies are used in order to show the results with the different values of a_g . P- Δ effects are
13 mostly significant for low values of peak ground acceleration. According to the comparison
14 in Fig. 10, for $a_g = 0.15$ g most of the structures collapse, because the displacement demand is
15 too high, i.e. dynamic instability occurs. As shown in Table 3, in design approaches no. 3 and
16 4 structural stiffness is generally influenced by the DL limit state. For low values of peak
17 ground acceleration, column sections are quite small because of the low values of the seismic
18 forces. If larger values of a_g are considered, the DL limit state becomes more severe, while
19 second order effects are less important. It is interesting noting that if design approach no. 4 is
20 used with modeling a, all the case studies exhibit a safe seismic response even if P- Δ effects
21 are neglected in the design of the column strength. Fig. 11 shows the ductility demands along
22 with the stability factors for all the case studies, designed with the four design approaches:
23 the differences between the approaches are negligible as well as the influence of the stability
24 factor (i.e., P- Δ effects influence). The overstrength due to seismic details and materials

1 properties significantly increases the structure strength and this effect compensates the
2 increase of the displacement demand on the structure due to the geometric nonlinearities.

3 **When are P- Δ effects important?**

4 In the previous sections, the code design approach is investigated by considering the
5 provisions for the geometric nonlinearities. In order to summarize the analyses results, Fig.
6 12 shows the ductility demand versus the stability factor for all the case studies, designed
7 with the first three design approaches (nos. 1, 2 and 3) and the three peak ground
8 accelerations. The results are obtained with analyses of first (gray markers) and second order
9 (black circles) by adopting the modeling approach c. The ductility capacity is also reported in
10 the same figure with a dashed black line. Most of the structures exhibit ductility demand in
11 terms of displacement very close to the capacity value. The distribution of the ductility
12 demand is very similar for the four height values and it can lead some interesting conclusions.
13 Since the considered approaches provide the amplification of the seismic effect if $\theta > 0.1$, it
14 can be stated that the amplification rule can take into account P- Δ effects and it generally
15 gives a safe response of the structure. However, the results show that the amplification is
16 necessary even if $\theta < 0.1$, since second order effects produces an increase in the ductility
17 demand which is not negligible. The largest differences between first and second order
18 analyses are recorded if the stability factor is in the range (0.2-0.3) and for low height: in
19 these cases, the influence of the flexibility on the displacement demand can justify the results.
20 For very large values of the stability factor ($\theta > 0.4$), the ductility demands of the first and
21 second order analyses are very similar. In these cases, the very large values of the
22 amplification factor α compensate the neglected geometric nonlinearities and the structures
23 are still in the elastic range, i.e. ductility close to 1.0.

24 Fig. 13 shows the ductility demand versus the stability factor for all the case studies, designed
25 with the first three design approaches (nos. 1, 2 and 3) and the three peak ground

1 accelerations. The results are obtained by using the modelling approach a. The differences
2 between first order and second order analysis are negligible for any value of the stability
3 factor. However, it is worth noting that the largest difference is recorded if the stability factor
4 is lower than 0.1: in these cases, code provisions influence the design in terms of minimum
5 reinforcement ratio (1%), making significant the section dimension variation, caused by the
6 different design approaches. Moreover, the influence of the overstrength is again
7 demonstrated by the low value of ductility: most of the structures are still in the elastic range.

8 **CONCLUSIONS**

9 The aim of the study is to assess the current design approaches, with particular focus to
10 Eurocode 8, to take into account geometric nonlinearities in precast single-story structures. A
11 parametric study is performed on several precast structures designed according to Eurocodes
12 by varying the height of the columns and the vertical axial load. In order to establish the main
13 influenced parameters of the seismic response of the investigated structure, nonlinear
14 dynamic analyses are performed by both neglecting and considering P- Δ effects. Both
15 strength and stiffness degradation were not considered in the plastic hinge hysteresis. The
16 comparison of the analyses results shows that the ductility demand in terms of displacement
17 is the main parameter in order to represent the influence of the geometric nonlinearities.
18 Therefore, in the study, the safety of the structures is assessed by comparing the displacement
19 ductility demand with the capacity. The results of the nonlinear dynamic analyses with the
20 second order effects demonstrate that the current design approach provides very low ductility
21 demand for the structures. This result is mainly caused by two factors: the difference between
22 the design period and the period in the analyses and the structural overstrength, due to
23 seismic details and the materials overstrength. The influence of the prescriptions on second
24 order effects are investigated and the following conclusions are drawn.

- 25 • Amplification of seismic effects is necessary even if $\theta < 0.1$.

- 1 • Both the code limitation on the minimum column section if $\theta > 0.1$ and the limit of the
2 stability factor (0.3) do not increase the structural safety with respect to the seismic
3 actions.
- 4 • If the structural design is performed by neglecting the limitations on both θ and the
5 column section, the structural safety is still guaranteed by amplifying the seismic
6 effects by α .
- 7 • If P- Δ effects are totally neglected in the design phase, structural safety can be
8 insufficient.

9 Finally, it should be noted that the above mentioned results can be also applicable to other
10 building codes with a similar approach to P- Δ effects, such as ASCE 7, providing that the
11 structural typology is similar and the considered structure falls within the parametric study
12 described herein. The study does not model the effect of the additional rotation at the column
13 base due to the foundation system; therefore, the presented outcomes can be applied to
14 buildings with adequate column-to-foundation connections.

15 **ACKNOWLEDGEMENTS**

16 This study was funded by both the Italian Department of Civil Protection in the frame of the
17 national project DPC - ReLUIIS 2015. The passionate support of Eng. Antonella Guerra to the
18 execution of the analyses is gratefully acknowledged.

19 **REFERENCES**

- 20 1. Belleri A, Brunesi E, Nascimbene R, Pagani M, Riva P, "Seismic Performance of
21 Precast Industrial Facilities Following Major Earthquakes in the Italian Territory," *Journal of*
22 *Performance of Constructed Facilities*, V. 29, No. 5, 2015, pp. 04014135.

- 1 2. Bournas DA, Negro P, Taucer FF, "Performance of industrial buildings during the
2 Emilia earthquakes in Northern Italy and recommendations for their strengthening," *Bulletin*
3 *of Earthquake Engineering*, V. 12, No. 5, 2014, pp. 2383-404.
- 4 3. Magliulo G, Ercolino M, Petrone C, Coppola O, Manfredi G, "The Emilia
5 Earthquake: the Seismic Performance of Precast Reinforced Concrete Buildings," *Earthquake*
6 *Spectra*, V. 30, No. 2, 2014, pp. 891-912.
- 7 4. Paulay T, "A consideration of P-Delta effects in ductile reinforced concrete frames,"
8 *Bulletin of the New Zealand national society for earthquake engineering*, V. 11, No. 3, 1978,
9 pp. 151-60.
- 10 5. Moss PJ, Carr AJ, "The effects of large displacements on the Earthquake Reponse of
11 Tall Structures," *Bulletin of the New Zealand national society for earthquake engineering*, V.
12 13, No. 4, 1981, pp. 317-20.
- 13 6. Bernal D, "Amplification factors for inelastic dynamic P- Δ effects in earthquake
14 analysis," *Earthquake Engineering and Structural Dynamics*, V. 15, 1987, pp. 635-51.
- 15 7. MacRae GA, "P- Δ effects on single-degree-of-freedom structures in earthquakes,"
16 *Earthquake Spectra*, V. 10, 1994, pp. 539-68.
- 17 8. Amara F, Bosco M, Marino EM, Rossi PP, "An accurate strength amplification factor
18 for the design of SDOF systems with P- Δ effects," *Earthquake Engineering and Structural*
19 *Dynamics*, V. 43, 2014, pp. 589-611.
- 20 9. Humar J, Mahgoub M, Ghorbanie-Asl M, "Effect of second-order forces on seismic
21 response," *Canadian Journal of Civil Engineering*, V. 33, No. 6, 2006, pp. 692-706.
- 22 10. Aschheim M, Montes EH, "The representation of P-Delta effects using yield point
23 spectra," *Engineering Structures*, V. 25, No. 11, 2003, pp. 1387-96.
- 24 11. CEN, "Design of structures for earthquake resistance, part 1," *Eurocode 8*, V.
25 Brussels, 2005.

- 1 12. American Society of Civil Engineers, "ASCE/SEI 7-10: Minimum Design Loads for
2 Buildings and Other Structures," Reston, Virginia, US, 2010.
- 3 13. Osanai Y, Watanabe F, Okamoto S, "Stress transfer mechanism of socket base
4 connections with precast concrete columns," *Aci Structural Journal*, V. 93, No. 3, 1996, pp.
5 266-76.
- 6 14. Negro P, Toniolo G, "Design Guidelines for Connections of Precast Structures under
7 Seismic Actions," *Joint Research Centre of the European Commission*, 2012.
- 8 15. CEN, "Eurocode 2: Design of concrete structures - Part 1-1: General rules and rules
9 for buildings. EN 1992-1-1," Brussels, Belgium, 2004.
- 10 16. DM 14/01/2008, "Norme tecniche per le costruzioni," *Roma, Italia, Gazzetta*
11 *Ufficiale*.
- 12 17. Brunesi E, Nascimbene R, Bolognini D, Bellotti D, "Experimental investigation of the
13 cyclic response of reinforced precast concrete framed structures," *PCI Journal*, V. 60, No. 2,
14 2015, pp. 57-79.
- 15 18. Andrews AL, "Slenderness Effects in Earthquake Resisting Frames," *Bulletin of the*
16 *New Zealand national society for earthquake engineering*, V. 10, No. 3, 1977, pp. 154-8.
- 17 19. Zhao J, Sritharan S, "Modeling of strain penetration effects in fiber-based analysis of
18 reinforced concrete structures," *Aci Structural Journal*, V. 104, No. 2, 2007, pp. 133-41.
- 19 20. Mander JB, Priestley MJN, Park R, "Theoretical Stress-Strain Model for Confined
20 Concrete," *Journal of Structural Engineering-Asce*, V. 114, No. 8, 1988, pp. 1804-26.
- 21 21. Fardis MN, Biskins DE, "Deformation capacity of RC members, as controlled by
22 flexure or shear," *In: Kabeyasawa T, Shiohara H (eds) Performance-based engineering for*
23 *earthquake resistant reinforced concrete structures, a volume honoring Shunsuke Otani,*
24 *University of Tokyo*, 2003.

- 1 22. CEN, "Eurocode 8: design of structures for earthquake resistance - Part 2: Bridges.
2 EN 1998-2," Brussels, Belgium., 2003.
- 3 23. Fardis MN, "Seismic design, assessment and retrofitting of concrete buildings based
4 on EN-Eurocode 8," 2009.
- 5 24. Zoubek B, Fischinger M, Isakovic T, "Estimation of the cyclic capacity of beam-to-
6 column dowel connections in precast industrial buildings," *Bulletin of Earthquake*
7 *Engineering*, V. 13, No. 7, 2015, pp. 2145-68.
- 8 25. Magliulo G, Ercolino M, Cimmino M, Capozzi V, Manfredi G, "FEM analysis of the
9 strength of RC beam-to-column dowel connections under monotonic actions," *Construction*
10 *and Building Materials*, V. 69, 2014, pp. 271-84.
- 11 26. Magliulo G, Ercolino M, Cimmino M, Capozzi V, Manfredi G, "Cyclic shear test on a
12 dowel beam-to-column connection of precast buildings," *Earthquake and Structures*, V. 9,
13 No. 3, 2015, pp. 541-62.
- 14 27. Rodrigues H, Varum H, Arêde A, Costa A, "Comparative efficiency analysis of
15 different nonlinear modelling strategies to simulate the biaxial response of RC columns,"
16 *Earthquake Engineering and Engineering Vibration*, V. 11, No. 4, 2012, pp. 553-66.
- 17 28. Magliulo G, Ramasco R, "Seismic response of three-dimensional r/c multi-storey
18 frame building under uni- and bi-directional input ground motion," *Earthquake Engineering*
19 *and Structural Dynamics*, V. 36, No. 12, 2007, pp. 1641-57.
- 20 29. SIMQKE, "Simulation of Earthquake Ground Motions," 2008.
- 21 30. Chopra AK, "Dynamics of structures: Theory and Applications to Earthquake
22 Engineering." Englewood Cliffs, New Jersey, USA: Prentice Hall; 1995.
- 23 31. The MathWorks Inc., "MATLAB Release 2015a," Natick, Massachusetts, United
24 States, 2015.

TABLES AND FIGURES

List of Tables:

Table 1 - Summary of European provisions for second order effects.

Table 2 - Summary of the four design approaches: the adopted or not adopted design provisions

Table 3 - Summary of different design approaches: h is the cross-section dimension, ρ is the reinforcement ratio, θ is the coefficient of stability (1 t=2204.62 lb and 1 m=3.28 ft)

List of Figures:

Fig. 1 - Precast structure

Fig. 2 - Equivalent SDOF system

Fig. 3 - Moment-rotation curves: comparison between modeling approaches

Fig. 4 - Average spectrum of the records (blue line) and design elastic spectrum (black line)

Fig. 5 - Force-displacement curve for first and second order analysis

Fig. 6 - Force-displacement curve for one case study with (black solid line) and without (gray solid line) P- Δ effects (1 kN=223.1 lb and 1 m=3.28 ft)

Fig. 7 – Comparison between modelling approaches: ductility demand for the investigated case studies, designed according to design approach no. 1 (1 t=2204 lb and 1 m=3.28 ft)

Fig. 8 - Displacement ductility demand vs mass values: comparison between design approaches no. 1 (blue line) and no. 2 (red line) (1 t=2204 lb). The nonlinear analyses are performed with the modelling approach c.

Fig. 9 - Displacement ductility demand vs mass values: comparison between design approaches no. 1 (blue line) and no. 3 (red line) (1 t=2204 lb). The nonlinear analyses are performed with the modelling approach c.

Fig. 10 - Displacement ductility demand vs mass values: comparison between design approaches no. 1 (blue line) and no. 4 (red line) (1t=2204 lb). The nonlinear analyses are performed with the modelling approach c.

Fig. 11 - Ductility demand in terms of displacement for all the case studies modelled with approach a.

Fig. 12 - Comparison between the ductility demand in the analysis of first (gray markers) and second order (black circles). The nonlinear analyses are performed with the modelling approach c.

Fig. 13 - Comparison between the ductility demand in the analysis of first (gray markers) and second order (black circles). The nonlinear analyses are performed with the modelling approach a.

Table 1 - Summary of European provisions for second order effects.

θ	EC8 provisions
$\theta \leq 0.1$	Second order effects not taken into account
$0.1 < \theta$	Seismic action effects amplified by a factor $\alpha = 1/(1 - \theta)$
≤ 0.2	Cross-section dimensions larger than 0.1 times the shear span
$0.2 < \theta$	Cross-section dimensions larger than 0.1 times the shear span
< 0.3	
≥ 0.3	The structure must be designed again

Table 2 - Summary of the four design approaches: the adopted or not adopted design provisions

Design rule	Design no. 1	Design no. 2	Design no. 3	Design no. 4
If $\theta \leq 0.1$, second order effects are not taken into account	✓	✓	✓	✓
If $\theta > 0.1$, seismic effects are amplified by α factor	✓	✓	✓	
If $\theta > 0.3$, the column section is increased	✓	✓		
If $\theta > 0.1$, limit on minimum column section is adopted (H/10)	✓			

Table 3 - Summary of different design approaches: h is the cross-section dimension, ρ is the reinforcement ratio, θ is the coefficient of stability (1 t=2204.62 lb and 1 m=3.28 ft)

$a_g = 0.15 \text{ g}$													
		Design approach no. 1				Design approach no. 2				Design approach no. 3			
		H [m]											
m [t]		6 m	8 m	10 m	12 m	6 m	8 m	10 m	12 m	6 m	8 m	10 m	12 m
10	h [m]	0.45	0.50	0.55	0.60	0.40	0.40	0.40	0.45	0.40	0.40	0.40	0.40
	ρ [%]	1.19	1.29	1.06	1.12	1.51	1.51	1.51	1.19	1.51	1.51	1.51	1.51
	θ [-]	0.07	0.08	0.08	0.08	0.11	0.19	0.30	0.27	0.11	0.19	0.30	0.43
70	h [m]	0.60	0.80	0.90	0.95	0.55	0.60	0.65	0.75	0.50	0.50	0.55	0.60
	ρ [%]	1.12	1.01	1.13	1.07	1.06	1.12	1.19	1.00	1.29	1.61	1.66	1.79
	θ [-]	0.15	0.08	0.08	0.09	0.21	0.26	0.30	0.24	0.31	0.54	0.58	0.59
130	h [m]	0.60	0.80	1.00	1.10	0.60	0.70	0.80	0.85	0.55	0.60	0.65	0.70
	ρ [%]	1.12	1.01	1.06	1.06	1.12	1.15	1.01	1.04	1.33	1.12	1.52	1.86
	θ [-]	0.27	0.15	0.10	0.10	0.27	0.26	0.24	0.27	0.39	0.49	0.55	0.59
$a_g = 0.25 \text{ g}$													
10	h [m]	0.45	0.50	0.55	0.60	0.40	0.40	0.45	0.45	0.40	0.40	0.45	0.45
	ρ [%]	1.19	1.29	1.06	1.12	1.51	1.51	1.19	1.19	1.51	1.51	1.19	1.19
	θ [-]	0.07	0.08	0.08	0.08	0.11	0.19	0.18	0.27	0.11	0.19	0.18	0.27
70	h [m]	0.65	0.80	0.90	0.95	0.65	0.70	0.70	0.75	0.65	0.70	0.70	0.75
	ρ [%]	1.19	1.01	1.13	1.07	1.19	1.15	1.15	1.00	1.19	1.15	1.15	1.00
	θ [-]	0.11	0.08	0.08	0.09	0.11	0.14	0.22	0.24	0.11	0.14	0.22	0.24
130	h [m]	0.75	0.80	1.00	1.10	0.75	0.80	0.85	0.85	0.75	0.80	0.85	0.85
	ρ [%]	1.35	1.01	1.06	1.06	1.35	1.01	1.04	1.04	1.35	1.01	1.04	1.04
	θ [-]	0.11	0.15	0.10	0.10	0.11	0.15	0.19	0.27	0.11	0.15	0.19	0.27
$a_g = 0.35 \text{ g}$													
10	h [m]	0.45	0.50	0.55	0.60	0.45	0.50	0.55	0.55	0.45	0.50	0.55	0.55
	ρ [%]	1.19	1.29	1.06	1.12	1.19	1.29	1.06	1.06	1.19	1.29	1.06	1.06
	θ [-]	0.07	0.08	0.08	0.08	0.07	0.08	0.08	0.12	0.07	0.08	0.08	0.12
70	h [m]	0.75	0.80	0.90	0.95	0.75	0.80	0.85	0.90	0.75	0.80	0.85	0.90
	ρ [%]	1.35	1.01	1.13	1.07	1.35	1.01	1.04	1.13	1.35	1.01	1.04	1.13
	θ [-]	0.06	0.08	0.08	0.09	0.06	0.08	0.10	0.12	0.06	0.08	0.10	0.12
130	h [m]	0.85	0.90	1.00	1.10	0.85	0.90	0.95	1.00	0.85	0.90	0.95	1.00
	ρ [%]	1.57	1.13	1.06	1.06	1.57	1.13	1.07	1.06	1.57	1.13	1.07	1.06
	θ [-]	0.07	0.10	0.10	0.10	0.07	0.10	0.12	0.14	0.07	0.10	0.12	0.14

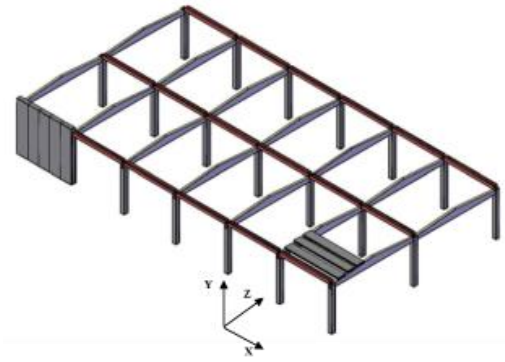


Fig. 1 - Precast structure

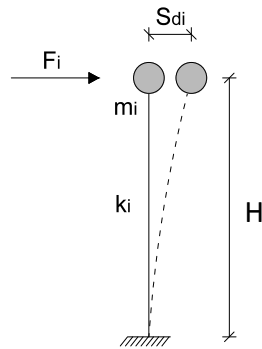


Fig. 2 - Equivalent SDOF system

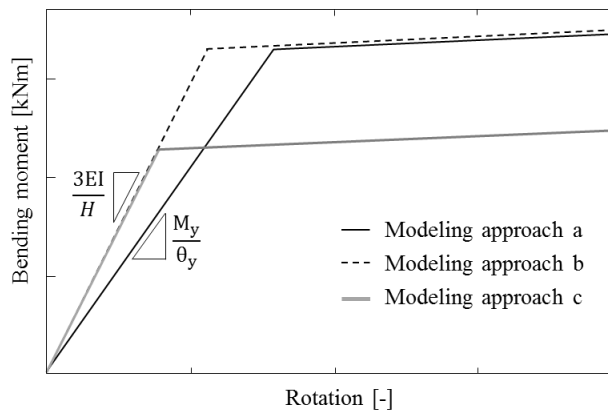


Fig. 3 - Moment-rotation curves: comparison between modeling approaches

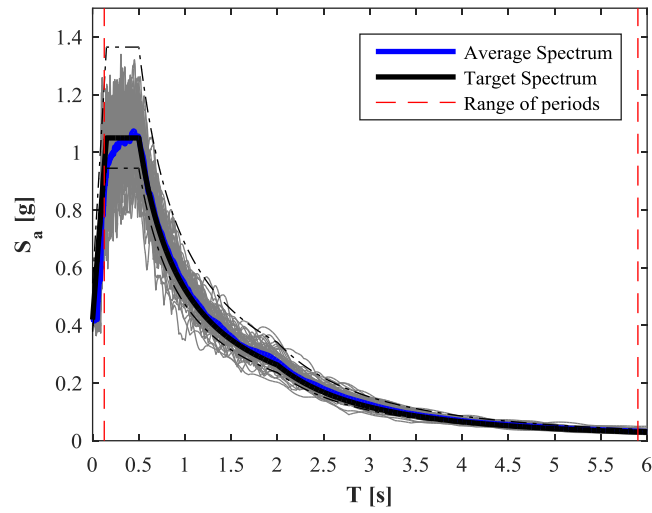


Fig. 4 - Average spectrum of the records (blue line) and design elastic spectrum (black line)

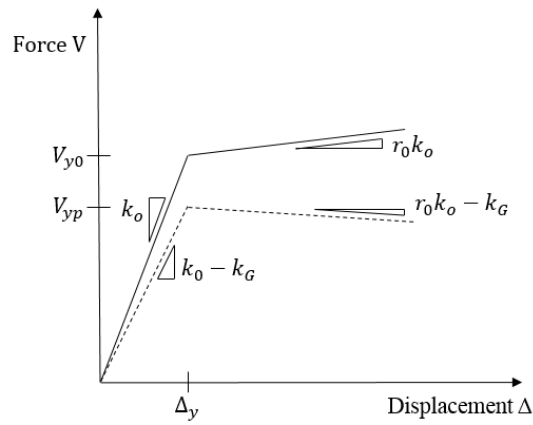


Fig. 5 - Force-displacement curve for first and second order analysis

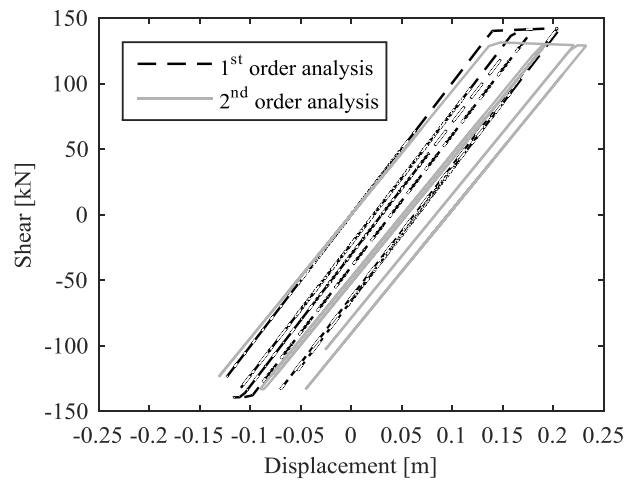


Fig. 6 - Force-displacement curve for one case study with (black solid line) and without (gray solid line) P-Δ effects (1 kN=223.1 lb and 1 m=3.28 ft)

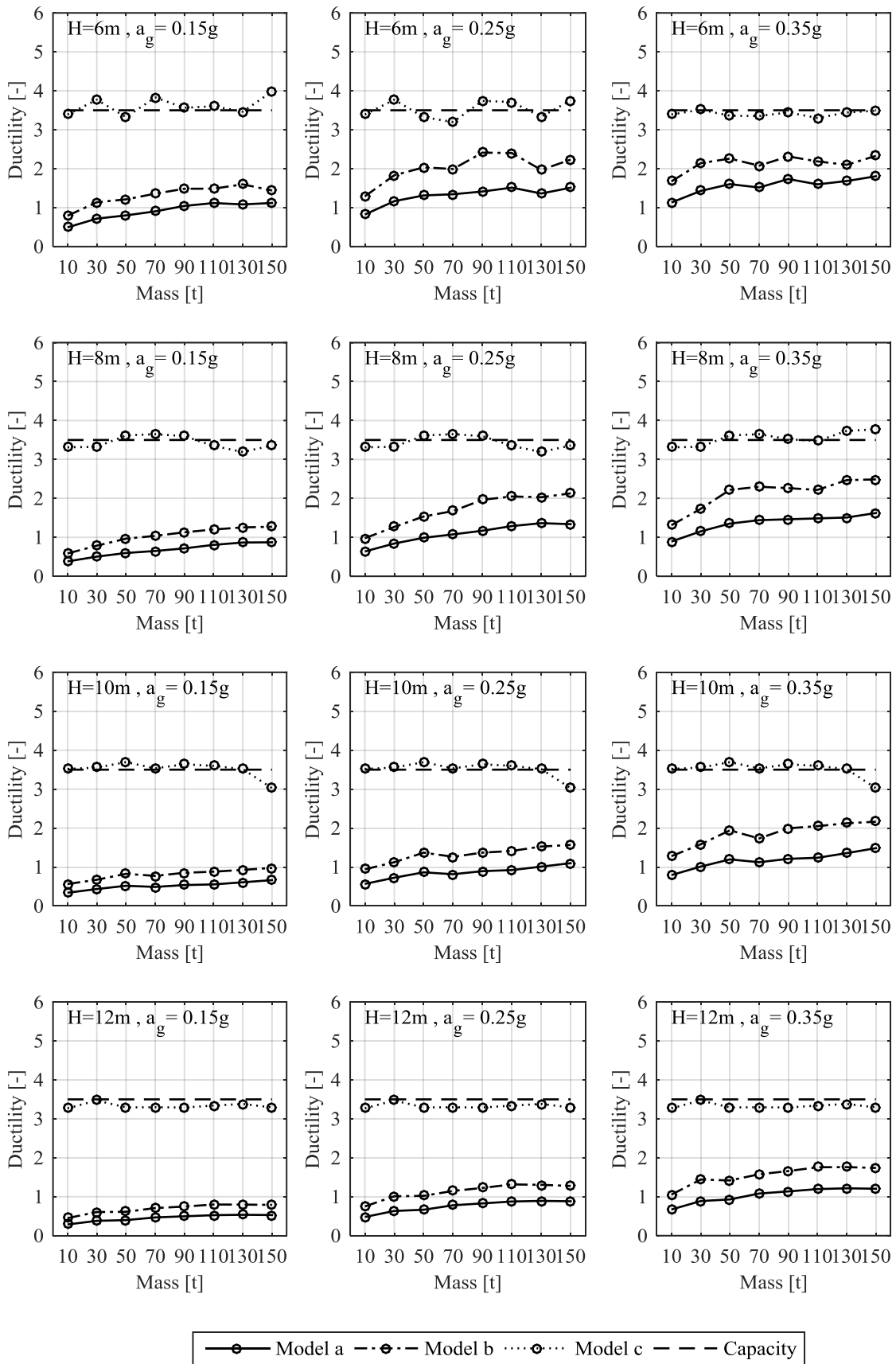


Fig. 7 – Comparison between modelling approaches: ductility demand for the investigated case studies, designed according to design approach no. 1 (1 t=2204 lb and 1 m=3.28 ft)

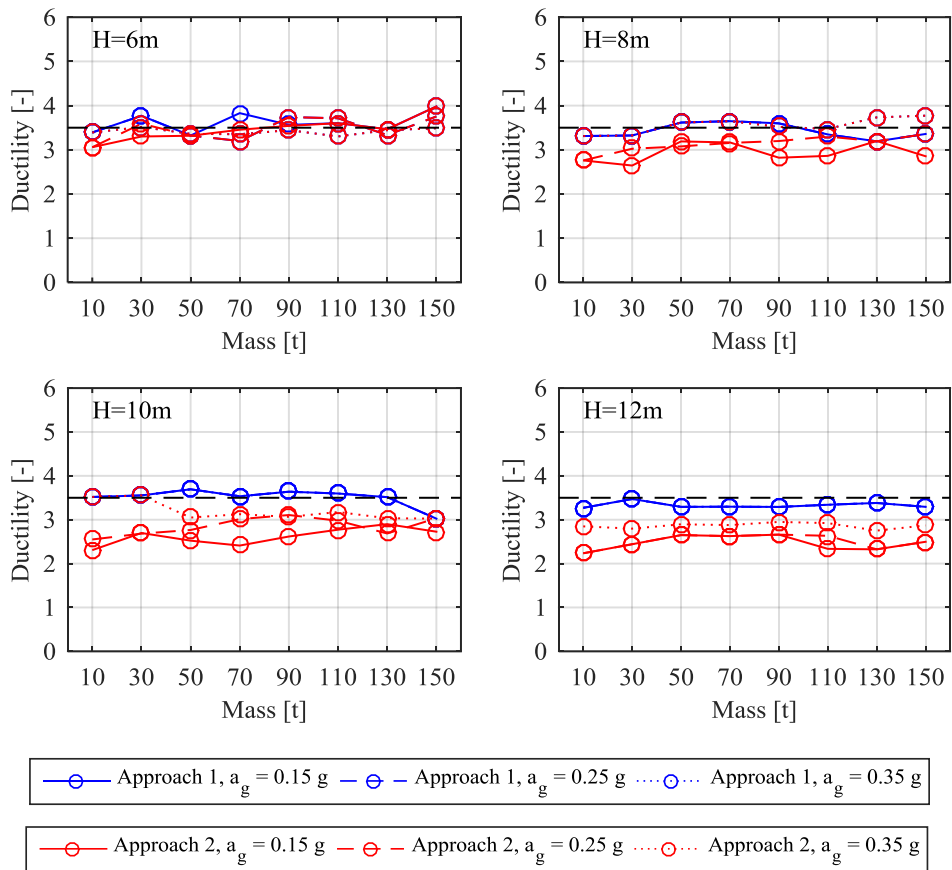


Fig. 8 - Displacement ductility demand vs mass values: comparison between design approaches no. 1 (blue line) and no. 2 (red line) (1 t=2204 lb). The nonlinear analyses are performed with the modelling approach c.

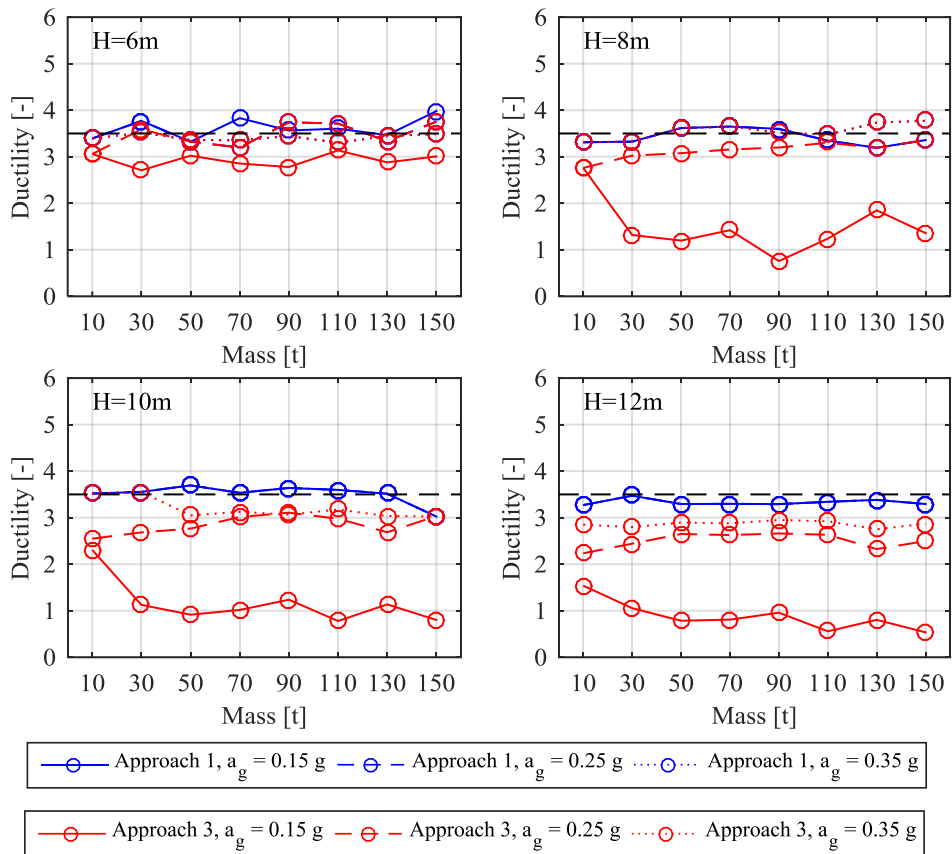


Fig. 9 - Displacement ductility demand vs mass values: comparison between design approaches no. 1 (blue line) and no. 3 (red line) (1 t=2204 lb). The nonlinear analyses are performed with the modelling approach c.

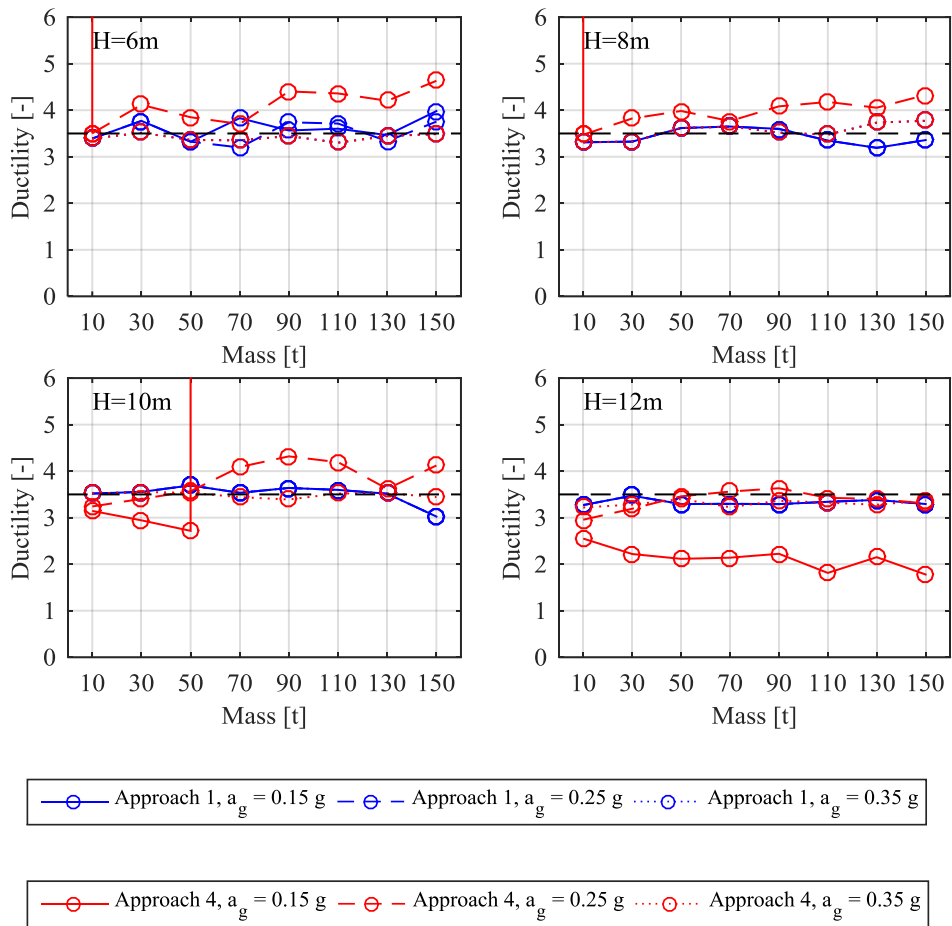


Fig. 10 - Displacement ductility demand vs mass values: comparison between design approaches no. 1 (blue line) and no. 4 (red line) (1t=2204 lb). The nonlinear analyses are performed with the modelling approach c.

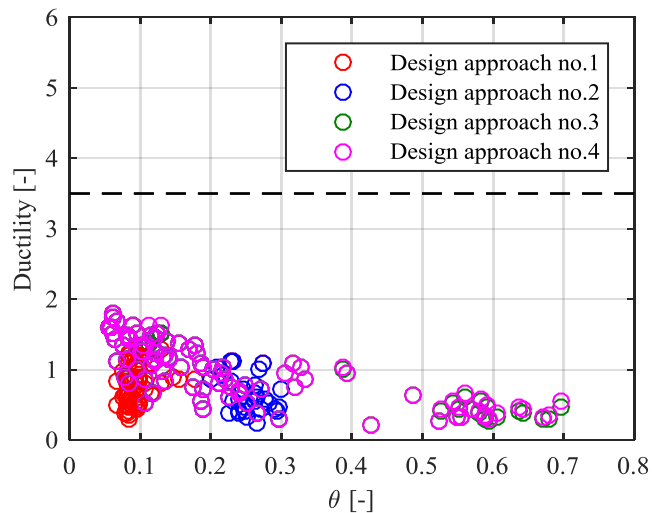


Fig. 11 - Ductility demand in terms of displacement for all the case studies modelled with approach a.

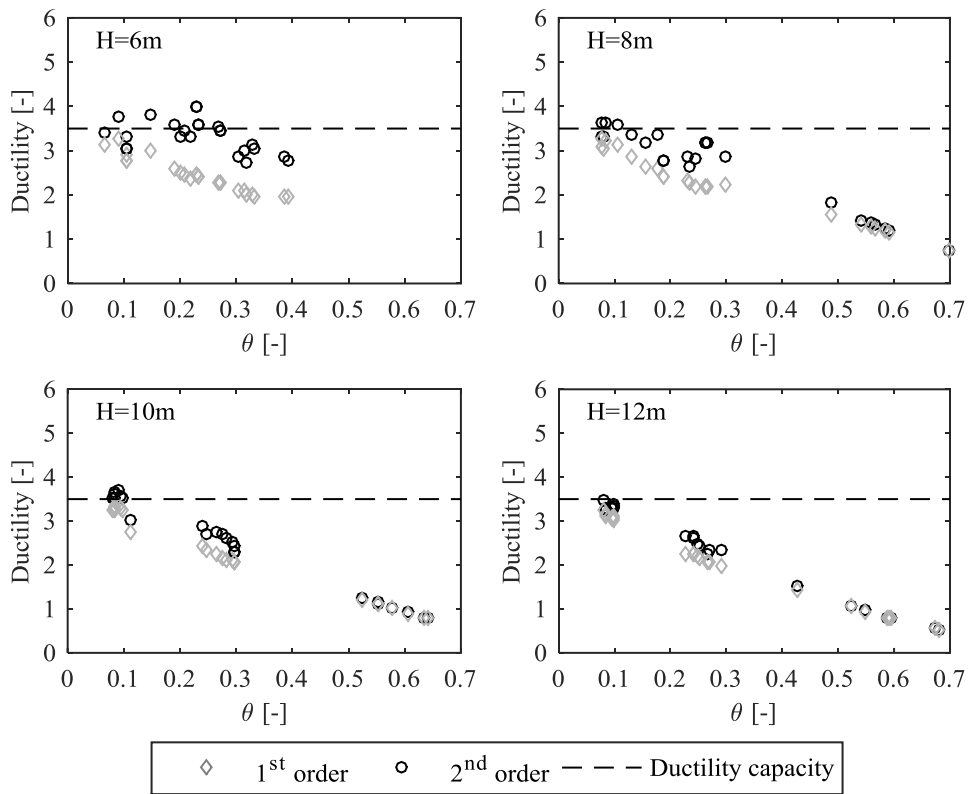


Fig. 12 - Comparison between the ductility demand in the analysis of first (gray markers) and second order (black circles). The nonlinear analyses are performed with the modelling approach c.

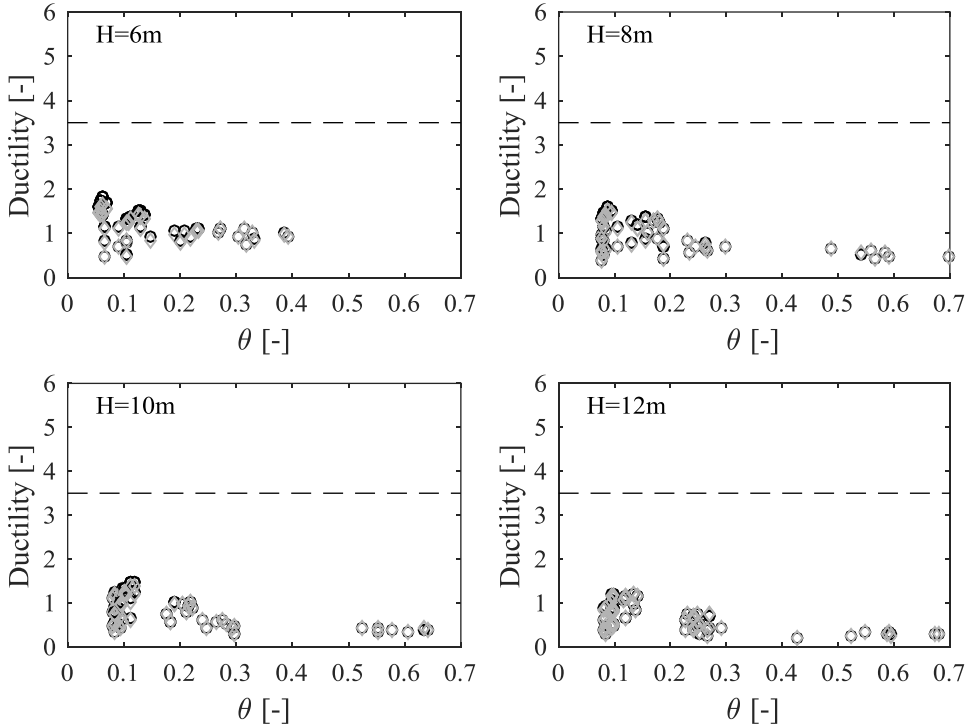


Fig. 13 - Comparison between the ductility demand in the analysis of first (gray markers) and second order (black circles). The nonlinear analyses are performed with the modelling approach a.